

# Entanglement in (1/2,1) mixed-spin XY model with long-range interactions

Seyit Deniz Han<sup>1</sup>, Tuğba Tüfekçi<sup>1</sup>, Timothy P. Spiller<sup>2</sup>, and Ekrem Aydiner<sup>1\*</sup>

<sup>1</sup>*Istanbul University Theoretical Physics Research Group, Istanbul University, Tr-34134, Istanbul, Turkey*

<sup>2</sup>*Quantum Information Science, School of Physics and Astronomy,  
University of Leeds, Leeds, LS2 9JT, United Kingdom*

(Dated: October 12, 2018)

In this study, considering the long-range interaction with an inverse-square and its trigonometric and hyperbolic variants in SCM model we investigate entanglement in (1/2,1) mixed-spin XY model. We also discuss the temperature and magnetic field dependence of the thermal entanglement in this system for different types of interaction. The numerical results show that, in the presence of the long-range interactions, thermal entanglement between spins has a rich behavior dependent upon the interaction strength, temperature and magnetic field. Indeed we find that for less than a critical distance there are entanglement plateaus dependent upon the distance between the spins, whereas above the critical distance the entanglement can exhibit sudden death.

PACS numbers: 03.65.Ud, 03.67.-a, 03.67.Hk, 75.10.Pq, 31.30.jh

## I. INTRODUCTION

Over the last decade or so, quantum entanglement has been recognized as crucial in various fields of quantum information [1] such as in quantum computation [2], quantum teleportation [3], superdense coding [4], quantum communication [5], quantum perfect state transfer [6], quantum cryptology [7, 8] and quantum computational speed-ups [9, 10]. Potential applications of entanglement in these fields have stimulated research on methods to quantify and control it. In the solid state arena, considerable attention has been devoted to interacting Heisenberg spin systems. Spins are recognized as candidates for solid state quantum computation [11–15] and even short range communication [16, 17]. Interactions such as Heisenberg enable gate operations in solid state quantum computation processors [11–15]. Therefore significant research has been performed to understand quantum entanglement behavior in spin systems, such as all various kinds of Heisenberg (XX, XY, XXZ and XYZ) models, and similarly Ising models. Many detailed and extensive investigations have addressed the dependence of entanglement on parameters such as magnetic field, single-ion anisotropy, temperature and interaction strength [18–42].

Recently, a new type of long-range interaction has been used in Refs. [43–45] to obtain long-distance entanglement in the spin system. In these works, spin pair interaction is given with a factor inversely proportional to a power of the distance between sites as  $J(R) \sim R^{-\alpha}$ . It is shown in these studies that long-distance entanglement can be obtained using this interaction type for different values of the interaction parameter  $\alpha$  in the Heisenberg spin systems. Here we must remark that this interaction type and its variants except the entanglement have been considered to explore many physical phenomena. Indeed, the inverse-square, trigonometric and hyperbolic

interacting particle systems [46–48] and its spin generalizations [49–52] are important model of many-body systems due to their exactly solvability and intimate connection to spin systems in condensed matter [49–59], and in the other areas in physics. These interaction types are called different names such as Haldane-Shastry models, Calogero-Moser or Sutherland-Calogero-Moser models or interactions in the literature. But, it is assumed that generalized Haldane-Shastry models is the supersymmetric partners of the Sutherland-Calogero-Moser type models. Hence, for historical reasons, in this study we will express these interactions as Sutherland-Calogero-Moser (SCM) model or SCM type interactions.

In this study, inspired by Refs. [43–45], we will consider long-range interaction with an inverse-square and its trigonometric and hyperbolic variants given in the SCM model to obtain entanglement between two spin in the mixed-spin (1/2,1) XY Heisenberg spin system. Our numerical results show that the long-range interactions lead to topological plateaus in entanglement. That is, the entanglement between spins still subsists throughout plateau up to critical distance although spins are separated from each other.

This paper is organized as follows. In Section II we define the mixed spin-1/2 and spin-1 XY model, and give the eigenvalues, eigenvectors, density matrix of the system and definition of negativity as a measure of entanglement. In Section III, we present and discuss the numerical results of modeling, giving the negativity of the system for SCM types i.e. inverse-square and its trigonometric and hyperbolic variants with varying model parameters. Finally Section IV is devoted to conclusions.

## II. MODEL

The Hamiltonian for the isotropic mixed spin (1/2,1) Heisenberg XY spin chain under an applied magnetic

\* ekrem.aydiner@istanbul.edu.tr

field  $B$  is given by

$$H = \sum_i B(s_i^z + S_{i+1}^z) - J(R) \sum_i [s_i^x S_{i+1}^x + s_i^y S_{i+1}^y] \quad (1)$$

where  $J(R)$  is the spin interaction coupling which will be defined in terms of SCM interactions. Also  $s_i$  and  $S_i$  ( $i = 1, 2$ ) are spin operators of the spin-1/2 and spin-1 components, respectively. The basis vectors of the two-spin system defined in Eq. (1) are  $\{|-1/2, -1\rangle, |1/2, 0\rangle, |-1/2, 1\rangle, |1/2, -1\rangle, |-1/2, 0\rangle, |1/2, 1\rangle\}$ , where  $|s, S\rangle$  is the eigenstate of  $s^z$  and  $S^z$  with corresponding eigenvalues given by  $s$  and  $S$ , respectively. The corresponding eigenvalues and eigenvectors of  $H$  for all  $J(R)$  can be given as follows

$$H |-1/2, -1\rangle = -3/2B |-1/2, -1\rangle \quad (2a)$$

$$H |1/2, 1\rangle = 3/2B |1/2, 1\rangle \quad (2b)$$

$$H |\phi^\pm\rangle = W_\pm |\phi^\pm\rangle \quad (2c)$$

$$H |\psi^\pm\rangle = Q_\pm |\psi^\pm\rangle \quad (2d)$$

where

$$\phi^\pm = 1/\sqrt{2}(|1/2, 0\rangle \pm |1/2, -1\rangle) \quad (3a)$$

$$\psi^\pm = 1/\sqrt{2}(|-1/2, 1\rangle \pm |-1/2, 0\rangle). \quad (3b)$$

Here  $\phi^\pm$  and  $\psi^\pm$  are maximally entangled states—so-called Bell states. The eigenstates of the isotropic XY model given by Eq. (2) with Eq. (3) do not change for different  $J(R)$  values. However, the eigenvalues  $W_\pm$  and  $Q_\pm$  in Eq. (2) do change dependent upon the value of  $J(R)$ . Each eigenvalue, for different types of the SCM interaction, will be explored in detail in the next section.

The partial transpose of the density matrix  $\rho$  for the two-spin which is defined by Eq. (1) is written in the form

$$\rho^{T_1} = \begin{pmatrix} a_{11} & a_{12} & 0 & 0 & 0 & 0 \\ a_{21} & a_{22} & 0 & 0 & 0 & 0 \\ 0 & 0 & a_{33} & 0 & 0 & 0 \\ 0 & 0 & 0 & a_{44} & 0 & 0 \\ 0 & 0 & 0 & 0 & a_{55} & a_{56} \\ 0 & 0 & 0 & 0 & a_{65} & a_{66} \end{pmatrix} \quad (4)$$

where  $a_{ij}$  ( $i, j = 1, \dots, 6$ ) are matrix elements of  $\rho^{T_1}$ . For different cases of  $J$ , the matrix elements of  $\rho^{T_1}$  are presented, along with the negativity.

Negativity is a measure of the quantum entanglement appropriate for application to higher spins [60–62]. Therefore we will use the concept of negativity to study entanglement in (1/2,1) mixed-spin XY systems. The negativity can be obtained using the density operator of the quantum system. The state of a system at thermal equilibrium can be described by the density operator  $\rho(T) = \exp(-\beta H)/Z$ , where  $Z = \text{Tr}(\exp(-\beta H))$  is the partition function and  $\beta = 1/kT$  ( $k$  is Boltzmann's constant, which is set to unity  $k = 1$  hereafter for the sake of simplicity, and  $T$  is the temperature). By choosing an appropriate set of orthonormal product basis states

$\{|v_i v_j\rangle\} \equiv \{|v_i\rangle |v_j\rangle\}$  for the density operator, the partial transpose is defined by its matrix elements

$$\rho_{m\mu, n\nu}^{T_1} = \langle v_m v_\mu | \rho | v_n v_\nu \rangle = \rho_{m\nu, n\mu}. \quad (5)$$

The negativity of a state  $\rho$  is by definition

$$N = \sum_i |\mu_i| \quad (6)$$

where  $\mu_i$  is the negative eigenvalue of the partial transpose density matrix  $\rho^{T_1}$ . Here  $\rho^{T_1}$  is the partial transpose with respect to the first system. The negativity  $N$  is related to trace norm of  $\rho^{T_1}$  via

$$N = \frac{\|\rho^{T_1}\| - 1}{2} \quad (7)$$

where the trace norm of  $\rho^{T_1}$  is equal to the sum of the absolute values of the eigenvalues of  $\rho^{T_1}$ .

### III. RESULTS AND DISCUSSIONS

In this section in order to discuss entanglement we will compute the negativity to quantify entanglement for two-spin in the isotropic mixed-spin (1/2,1) XY Heisenberg spin chain given by Eq. (1) considering different long-range interaction types given in the SCM model [46–52]. Therefore, in the below Subsections, we will consider inverse-square interaction coupling  $J_0/R^2$  as type I, trigonometric interaction coupling  $J_0/\sin^2(R)$  as type II and hyperbolic interaction coupling  $J_0/\sinh^2(R)$  as type III in Subsections III.A,B and C respectively.

#### A. SCM Type I: $J(R) = J_0/R^2$

Firstly we consider the inverse-square interaction type in SCM model, which is defined with exchange interaction  $J(R) = J_0/R^2$  [46–52]. Here we set  $J_0 = 1$  for simplicity. The eigenvalues for this type of SCM interaction are given by

$$\pm 3B/2, \quad W_\pm = -\frac{B}{2} \pm \frac{\sqrt{2}}{2R^2}, \quad Q_\pm = \frac{B}{2} \pm \frac{\sqrt{2}}{2R^2}. \quad (8)$$

Using the eigenvalues in Eq. (8) and the eigenvectors in Eq. (2) (with Eq. (3)) the density matrix  $\rho$  can be constructed. For a SCM interaction of type  $J(R) = 1/R^2$ , the partial transpose of  $\rho$  shown in Eq. (4) has matrix

elements given in Eq. (9) as follows:

$$a_{11} = \frac{1}{Z} e^{\frac{3B}{2T}} \quad (9a)$$

$$a_{12} = a_{21} = -\frac{1}{Z} e^{\frac{B}{2T}} \sinh\left[\frac{1}{\sqrt{2}R^2T}\right] \quad (9b)$$

$$a_{22} = a_{33} = \frac{1}{Z} e^{-\frac{B}{2T}} \cosh\left[\frac{1}{\sqrt{2}R^2T}\right] \quad (9c)$$

$$a_{44} = a_{55} = \frac{1}{Z} e^{\frac{B}{2T}} \cosh\left[\frac{1}{\sqrt{2}R^2T}\right] \quad (9d)$$

$$a_{56} = a_{65} = -\frac{1}{Z} e^{-\frac{B}{2T}} \sinh\left[\frac{1}{\sqrt{2}R^2T}\right] \quad (9e)$$

$$a_{66} = \frac{1}{Z} e^{-\frac{3B}{2T}} \quad (9f)$$

where the partition function  $Z$  is written as

$$Z = 2 \left\{ \cosh\left[\frac{3B}{2T}\right] + 2 \cosh\left[\frac{B}{2T}\right] \cosh\left[\frac{1}{\sqrt{2}R^2T}\right] \right\}. \quad (10)$$

For the SCM interaction of type  $J(R) = 1/R^2$ , the negativity given by Eq. (7) for the two-spin system defined in the Heisenberg mixed XY model in Eq. (1) can be obtained from summation of the negative eigenvalues of the partial transpose matrix Eq. (4) with elements as in Eq. (9).

The negativity of the two-spin system in the case  $J(R) = 1/R^2$  is plotted versus  $R$  for different temperature  $T$  values at fixed magnetic field  $B = 1$  and for different magnetic field values at fixed temperature  $T = 1$ , in Fig. (1a) and Fig. (1b), respectively. Firstly we note that there is a singularity at  $R = 0$ , hence, as it can be seen from both figures that negativity drops to zero in the limit  $R \rightarrow 0$ . On the other hand, as it can be seen from Fig. (1a), the negativity reaches a plateau for small  $R$  at a fixed temperature  $T$  and fixed magnetic field  $B$ . The value of the negativity plateau is 0.5 at very low temperatures, decreasing at higher temperatures although with the plateau behavior still apparent. Similar behavior is observed in Fig. (1b), with the negativity attaining a plateau at small  $R$ . For relatively high magnetic fields the plateau value approaches 0.5, but decreases for lower magnetic values as expected. A very interesting aspect of the behavior in these figures is that the negativity shows this plateau behavior, like in topological quantization, dependent upon the distance between the two spins for different temperatures at fixed  $B$  and similarly for different magnetic fields at fixed temperature. It is interesting to note that the plateau width (in  $R$ ) increases as it approaches its maximum for lowering  $T$ , whereas the width decreases as it approaches its maximum for increasing  $B$ . In both figures, for increasing  $R$ , in some cases the negativity exhibits a form of sudden death [63–65], reaching zero at a critical  $R$  value of  $R_c$  [66]. The results of Fig. (1a) demonstrate the dependence of the critical  $R_c$  on temperature  $T$  at fixed  $B$ , whereas the results of Fig. (1b) demonstrate some insensitivity of  $R_c$  to magnetic field  $B$  at fixed  $T$  but with the entanglement slope (at  $R_c$ , as a function of  $R$ ) dependent upon  $B$ .

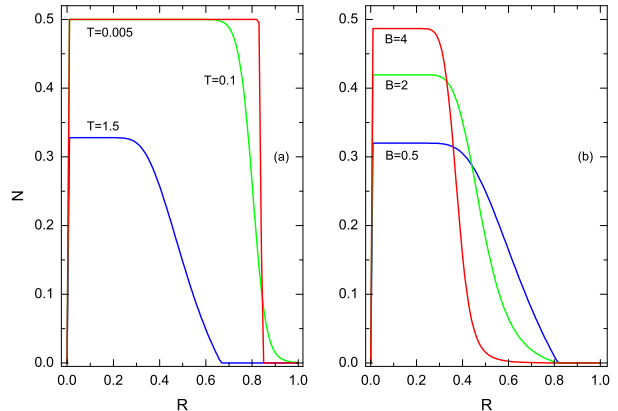


FIG. 1. Negativity as a function of  $R$  for the two-spin ferromagnetic XY system (a) for selected temperatures at fixed magnetic field  $B = 1$ , (b) for selected external uniform magnetic fields at fixed temperature  $T = 1$ .

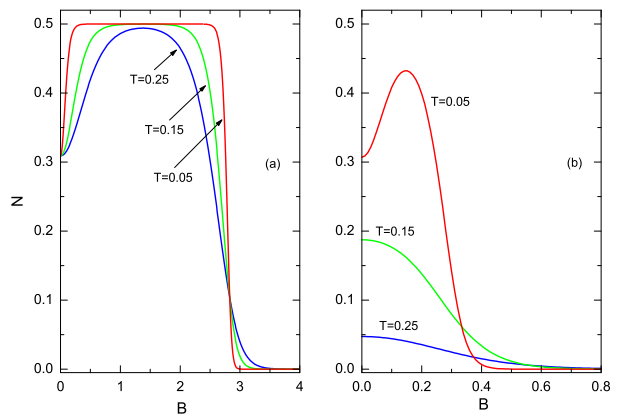


FIG. 2. Magnetic field dependence of negativity in the two-spin ferromagnetic XY system for selected temperatures (a) at fixed  $R = 0.5$ , (b) at fixed  $R = 1.5$ .

Here we express that the topological plateaus in Fig. (1) emerge from the presence of the long-range interaction with inverse-square  $1/R^2$  in this model.

In order to further investigate the magnetic field dependence of the entanglement for different  $R$  values in the larger  $R$  regime, the negativity is plotted as a function of magnetic field for different temperature values ( $T = 0.05, 0.15, 0.25$ ), at fixed  $R = 0.5$  in Fig. (2a), and at fixed  $R = 1.5$  in Fig (2b). It can be seen from these figures that although the negativity curves have different detailed characteristics, the negativity for the two different values of  $R$  tends to zero for increasing  $B$  values. Identifying a critical  $B_c$  beyond which there is no entanglement suggests that this critical  $B_c$  value and the manner in which the entanglement vanishes both depend

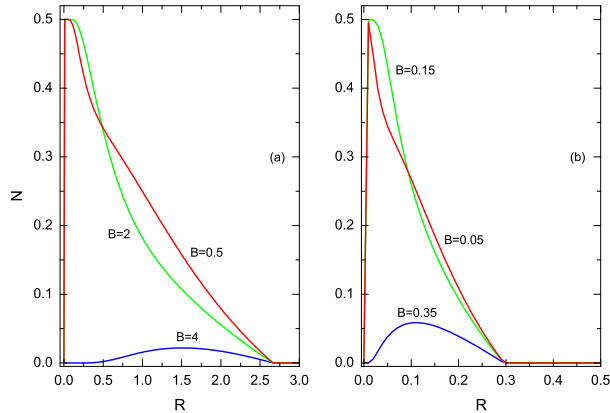


FIG. 3. Temperature dependence of the negativity in the two-spin ferromagnetic XY system for selected magnetic field values (a) at fixed  $R = 0.5$ , (b) at fixed  $R = 1.5$ .

upon the chosen  $R$  and the temperature  $T$ .

Similarly, to further investigate the temperature dependence of the entanglement for different  $R$  values in the larger  $R$  regime, the negativity is plotted versus temperature for different magnetic field values ( $B = 0.5, 2, 4$ ), at fixed  $R = 0.5$  in Fig. (3a), and for different magnetic field values ( $B = 0.05, 0.15, 0.35$ ) at fixed  $R = 1.5$  in Fig. (3b). Since the negativity does not appear for  $B = 0.5, 2, 4$  at  $R = 1.5$ , we plot Fig. (3b) for different  $B$  values. As it can be seen from these figures, the temperature dependence of the negativity for different  $R$  and  $B$  values has very similar characteristic behavior. In both figures, the negativity curves for different magnetic values meet at the same temperature point which indicates a critical temperature value  $T_c$ . Furthermore, Fig. (3) demonstrates critical temperature  $T_c$  dependence on  $R$ , consistent with the critical  $R_c$  dependence on  $T$  of Fig. (1a). Similarly to Fig. (1) singularity behavior in negativity appears in the limit  $R \rightarrow 0$  in Fig. (3).

To further demonstrate and unify the dependence of the entanglement on temperature and magnetic field, a surface plot of the negativity is given in Fig. (4), for an example fixed  $R = 0.5$ , as a function of both  $T$  and  $B$ . As can be seen from Fig. (4), the negativity of the two-spin XY system has a plateau for this fixed  $R$  value. We also know from the previous Figs. (1), (2) and (3) that the range of the plateau depends on magnetic field and temperature and we can qualitatively comment that range (in  $T$  and  $B$ ) of the plateau for small  $R$  values will be bigger than that for large  $R$  values. Furthermore, Fig. (4) shows clearly that for very low temperature values the negativity exhibits critical behavior (coming off the plateau) and decreases rapidly with increasing field at a critical magnetic field value. However, for higher temperatures beyond  $T_c$  when there is no access to the plateau, the negativity simply decreases smoothly for increasing magnetic field.

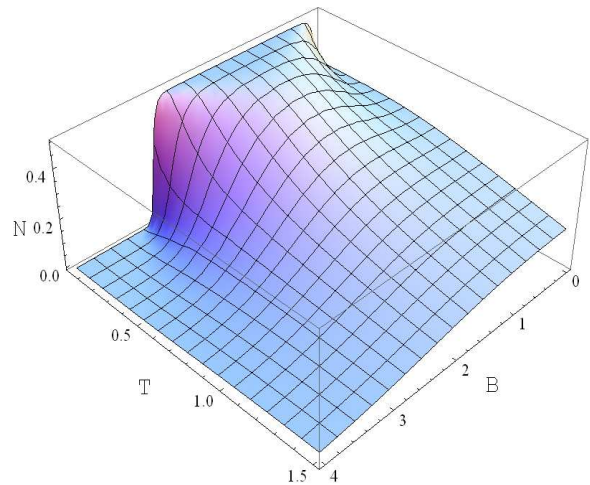


FIG. 4. Surface plot of the negativity in the two-spin ferromagnetic XY system as a function of temperature and magnetic field at fixed  $R = 0.5$

To summarize, in this subsection, we have investigated the behavior of the entanglement of a two-spin XY system in the case of long-range SCM interaction  $J(R) = 1/R^2$ . We have discussed the dependence of the negativity on interaction parameter  $R$ , magnetic field  $B$  and temperature  $T$ . We have shown that entanglement appears in the presence of the long-range interaction in some parameter regimes, and there is critical behavior in entanglement which suddenly deaths at critical values of interaction parameter, magnetic field and temperature.

### B. SCM Type II: $J(R) = J_0/\sin^2 R$

Secondly we consider trigonometric version of long-range interaction in SCM model, which is defined with exchange interaction  $J(R) = J_0/\sin^2 R$  [46–52]. Here we set  $J_0 = 1$  and  $\theta = R$  for simplicity. The eigenvalues for this type of SCM interaction are given by

$$\pm 3B/2, W_{\pm} = \frac{\mp B\varphi + 4\sqrt{\varphi}}{2\varphi}, Q_{\pm} = \frac{\mp B\varphi - 4\sqrt{\varphi}}{2\varphi} \quad (11)$$

where  $\varphi = 3 - 4\cos[2R] + \cos[4R]$ . Using the eigenvalues in Eq. (11) and the eigenvectors in Eq. (2) (with Eq. (3)) the density matrix  $\rho$  can be constructed. For the SCM interaction type of  $J(R) = 1/\sin^2 R$ , the partial transpose of  $\rho$  shown in Eq. (4) has matrix elements given in

Eq. (12) as follows:

$$a_{11} = \frac{1}{Z} e^{\frac{3B}{2T}} \quad (12a)$$

$$a_{12} = a_{21} = \frac{\mu_-}{2Z} (-e^{-\delta_1} + e^{-\delta_2}) \quad (12b)$$

$$a_{22} = a_{33} = \frac{\mu_+}{2Z} (e^{\delta_1} + e^{\delta_2}) \quad (12c)$$

$$a_{44} = a_{55} = \frac{\mu_-}{2Z} (e^{-\delta_1} + e^{-\delta_2}) \quad (12d)$$

$$a_{56} = a_{65} = \frac{\mu_+}{2Z} (e^{\delta_1} - e^{\delta_2}) \quad (12e)$$

$$a_{66} = \frac{1}{Z} e^{-\frac{3B}{2T}} \quad (12f)$$

where  $\delta_1 = \frac{B \cos[2R] \csc[R]^4}{2T}$ ,  $\delta_2 = \frac{B(3+\cos[4R]) \csc[R]^4}{8T}$  and  $\mu_{\mp} = \exp(\mp \frac{\csc[R]^4 (3B+4B \cos[2R]+B \cos[4R]+8\sqrt{2}\sqrt{\sin[R]^4})}{16T})$ . The partition function  $Z$  for the interaction type  $J = 1/\sin^2(R)$  can therefore be written as

$$Z = \mu_- e^{-(\delta_1+\delta_2)} \{ e^{\delta_1+2\delta_2} + e^{2\delta_1+\delta_2} + \mu_+ e^{\frac{5\delta_1-\delta_2}{2}} \quad (13) \\ + \mu_+^2 e^{\delta_2} + \mu_+ e^{\frac{-\delta_1+5\delta_2}{2}} + \mu_+^2 e^{\delta_1} \} .$$

For the SCM interaction of type  $J(R) = 1/\sin^2 R$ , the negativity given by Eq. (7) for the two-spin system defined in the Heisenberg mixed XY model in Eq. (1) can be obtained from summation of the negative eigenvalues of the partial transpose matrix Eq. (4) with elements as in Eq. (12).

The negativity for this  $J(R) = 1/\sin^2 R$  case is plotted versus  $R$  ( $0 \leq R \leq \pi$ ) for different temperature  $T$  values at fixed magnetic field value  $B$  in Fig. (5a), and for different magnetic field values at fixed temperature  $T$  in Fig. (5b). One can see that negativity drops to zero in the limit  $R \rightarrow 0$  and  $R \rightarrow \pi$  in both figures. In these limits, the negativity have two singularities. On the other hand, it can be seen from these figures that the negativity drops suddenly to zero with  $R$ , creating a valley symmetric about  $R = \pi/2$ . This occurs for a fixed  $B = 1$  value at the various temperature values used for Fig. (5a), with the valley width and side plateau heights dependent upon the chosen  $T$  value and lower  $T$  creating a narrower, higher-sided ( $N = 0.5$ ) valley. The effect also occurs for a fixed  $T = 1$  value at the various magnetic field values used for Fig. (5b), with the valley width and side plateau heights dependent upon the chosen  $B$  value and higher  $B$  creating a slightly wider, steeper-sided and higher-sided (approaching  $N = 0.5$ ) valley. Given the symmetric behavior of the negativity in the interval  $0 \leq R \leq \pi$ , as shown in Figs. (5) it is clear that there are two critical  $R_c$  values in these figures, equidistant from  $R = \pi/2$ .

In order to further demonstrate and unify the dependence of the entanglement on  $R$  ( $0 \leq R \leq \pi$ ) and  $T$ , the negativity surface is plotted as a function of  $R$  and  $T$  for a fixed value  $B = 1$  in Fig. (6). This surface plot shows the temperature dependence of the interesting valley behavior of the negativity, with side plateaus, as a function of  $R$ . It is clear that at this fixed value of  $B = 1$ , the negativity valley (symmetric in  $R$  about  $R = \pi/2$ ) widens

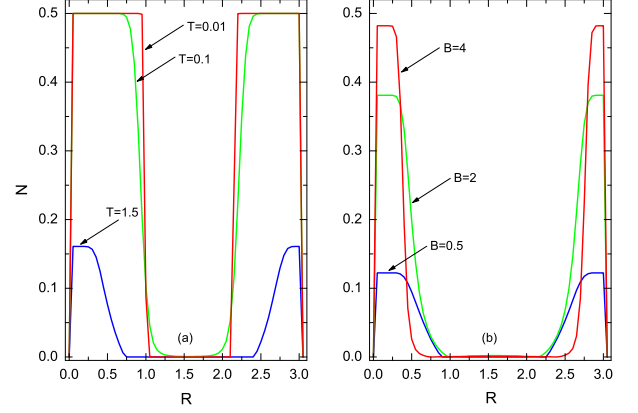


FIG. 5. Negativity as a function of  $R$  for the two-spin ferromagnetic XY system in the case  $J(R) = 1/\sin^2 R$  (a) for selected temperatures at fixed magnetic field  $B = 1$ , (b) for selected external uniform magnetic fields at fixed temperature  $T = 1$ .

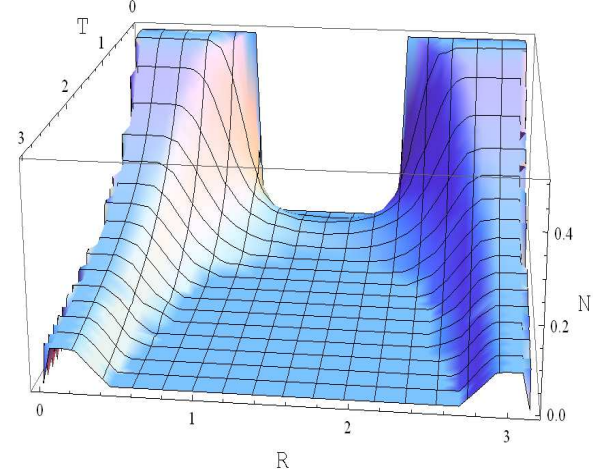


FIG. 6. Surface plot of the negativity for the two-spin ferromagnetic XY system in the case  $J(R) = 1/\sin^2 R$  as a function of temperature  $T$  and interaction parameter  $R$  at fixed  $B = 1$ .

with increasing temperature, with the side plateaus diminishing and dropping from their low  $T$  maximum of  $N = 0.5$ . The  $T$ -dependence of the two symmetric critical  $R_c$  values is clearly visible in this surface plot. However, whilst the valley profile of the negativity with  $R$  persists all the way down in  $T$  to zero temperature, it is clear that at the lowest temperatures the valley floor exhibits a ridge for which the negativity is non-zero for all values of  $R$  including the mid-point  $R = \pi/2$ . At these low temperatures critical behavior with  $N$  dropping suddenly to zero thus disappears, although the negativity still exhibits a critical change from the plateau at  $N = 0.5$  to the small finite value at the valley floor. The behavior of this low- $T$  ridge in negativity as the temperature actually

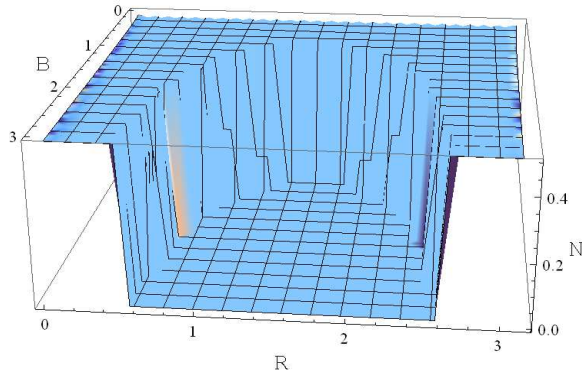


FIG. 7. Surface plot of the negativity for the two-spin ferromagnetic XY system in the case  $J(R) = 1/\sin^2 R$  as a function of magnetic field  $B$  and interaction parameter  $R$  at fixed  $T = 0.001$ .

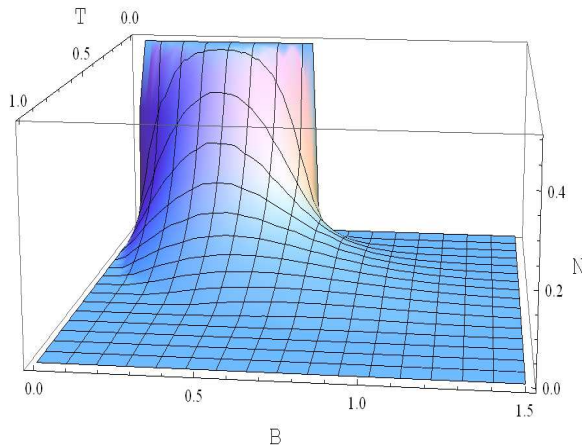


FIG. 8. Surface plot of the negativity for the two-spin ferromagnetic XY system in the case  $J(R) = 1/\sin^2 R$  as a function of temperature  $T$  and magnetic field  $B$  at fixed  $R = \pi/2$ .

approaches zero is dependent upon the fixed value of  $B$  chosen, and will be illustrated later in Fig. (8). Similarly to Fig. (5) singularity behavior in negativity appears in the limit  $R \rightarrow 0$  and  $R \rightarrow \pi$  in Fig. (6).

Similarly, in order to further demonstrate and unify the dependence of the entanglement on  $R$  ( $0 < R < \pi$ ) and  $B$ , the negativity surface is plotted as a function of  $R$  and  $B$  for a fixed value  $T = 0.001$  in Fig. (7). This surface plot shows the field dependence of the interesting valley behavior of the negativity, with side plateaus, as a function of  $R$ . It is clear that at this fixed value of  $T = 0.001$ , the negativity valley (symmetric in  $R$  about  $R = \pi/2$ ) widens with increasing temperature, with the side plateaus essentially remaining at their low  $B$  maximum of  $N = 0.5$ . The  $B$ -dependence of the two symmetric

critical  $R_c$  values is clearly visible in this surface plot and it is also clear that these merge at a specific  $B$  point and below this value of  $B$  the entanglement is at its maximum for all values of  $R$ , with no critical behavior.

The final figure for the SCM interaction  $J(R) = 1/\sin^2 R$  is Fig. (8), which shows the behavior with  $B$  and  $T$  of the negativity surface at a fixed value of  $R = \pi/2$ , which is the mid-point of the  $R$  range—about which the valley behavior in  $R$  in Fig. (6) and Fig. (7) is symmetric. It can be seen that non-zero negativity appears at low  $T$  for this fixed  $R = \pi/2$ , consistent with the ridge seen in Fig. (6). The behavior of the ridge (or valley floor) midpoint as a function of  $B$  and  $T$  is captured in Fig. (8). It can be seen from this that at very low and high magnetic field values, the negativity (and thus the ridge) disappears as  $T \rightarrow 0$  or may not even appear at all, whereas for intermediate  $B \sim 1/2$  the negativity (ridge) appears and grows as  $T \rightarrow 0$ .

As a result, in this subsection, we have investigated the behavior of the entanglement of a two-spin XY system in the case of the long-range SCM interaction  $J(R) = 1/\sin^2 R$ . We have discussed the dependence of the negativity on interaction parameter  $R$ , magnetic field  $B$  and temperature  $T$ . We have demonstrated the symmetric behavior about  $R = \pi/2$  (with singular behavior as  $R \rightarrow 0$  and  $R \rightarrow \pi$ ). The critical plateau and valley behavior is seen in significant parameter regimes along with the associated entanglement sudden death.

### C. SCM Type III: $J(R) = J_0/\sinh^2 R$

Finally we consider hyperbolic version of long-range interaction in SCM model, which is defined with exchange interaction  $J(R) = J_0/\sinh^2 R$  [46–52]. Here we set  $J_0 = 1$  and  $\theta = R$  for simplicity. The eigenvalues for this type of SCM interaction are given by

$$\begin{aligned} \pm 3B/2, \quad W_{\pm} &= \frac{1}{2} \left( \pm B + \frac{\sqrt{2}}{\sqrt{\sinh[R]^4}} \right), \\ Q_{\pm} &= \frac{1}{2} \left( \pm B - \frac{\sqrt{2}}{\sqrt{\sinh[R]^4}} \right). \end{aligned} \quad (14)$$

Using the eigenvalues in Eq.(14) and the eigenvectors in Eq. (2) (with Eq.(3)) the density matrix  $\rho$  can be constructed. For the SCM interaction type of  $J(R) = 1/\sinh^2 R$ , the partial transpose of  $\rho$  shown in Eq.(4)

has matrix elements given in Eq. (15) as follows:

$$a_{11} = \frac{1}{Z} e^{\frac{3B}{2T}} \quad (15a)$$

$$a_{12} = a_{21} = \frac{\eta}{2Z} (1 - e^{\frac{B}{T}}) \quad (15b)$$

$$a_{22} = a_{33} = \frac{\xi}{2Z} (1 + e^{\frac{B}{T}}) \quad (15c)$$

$$a_{44} = a_{55} = \frac{\eta}{2Z} (1 + e^{\frac{B}{T}}) \quad (15d)$$

$$a_{56} = a_{65} = \frac{\xi}{2Z} (1 - e^{\frac{B}{T}}) \quad (15e)$$

$$a_{66} = \frac{1}{Z} e^{-\frac{3B}{2T}} \quad (15f)$$

where  $\eta = \exp(-(B - \sqrt{2} \text{csch}[R]^4 \sqrt{\sinh[R]^4})/2T)$ ,  $\xi = \exp(-(B + \sqrt{2} \sqrt{\sinh[R]^4})/2T)$ . The partition function for this case is simply given as

$$Z = 2 \cosh\left[\frac{3B}{2T}\right] + (1 + e^{B/T})(\xi + \eta). \quad (16)$$

Similarly, the negativity follows from summation of the negative eigenvalues of the partial transpose density matrix Eq. (4) with elements as in Eq. (15).

The negativity for this  $J(R) = 1/\sinh^2 R$  case is plotted versus  $R$  ( $0 < R \leq \pi$ ) for different temperature  $T$  values at fixed magnetic field value  $B$  in Fig. (9a), and for different magnetic field values at fixed temperature  $T$  in Fig. (9b). It can be seen from Fig. (9a) that, at a fixed value of  $B = 1$ , the negativity attains its maximum value in a plateau for low temperature, dropping suddenly to zero with increasing  $R$  at a critical  $R_c$  value, but it also drops to zero in the limit  $R \rightarrow 0$ . In this  $R \rightarrow 0$  limit, the negativity has a singularity. The value of negativity on the plateau and the plateau width in  $R$  both vary with  $T$ , with the lowest value of  $T = 0.001$  exhibiting saturation at  $N = 0.5$ . Fig. (9b) also shows plateau behavior of negativity at small  $R$  with a sudden drop as  $R$  exceeds a threshold  $R_c$ . Similarly to Fig. (9a), in the limit  $R \rightarrow 0$ , a singularity appears in negativity. Negativity also drops to zero in this limit. However, for the fixed value  $T = 1$  chosen none of the plateau values for  $N$  attain the maximum, with the value at the plateau increasing with increasing magnetic field  $B$ . The plateau width in  $R$  is essentially independent of  $B$  for the range considered.

In order to further demonstrate and unify the dependence of entanglement on  $R$  and  $T$ , the negativity surface is plotted as a function  $R$  ( $-\pi \leq R \leq \pi$ ) and  $T$  for a fixed value of  $B = 1.5$  in Fig. (10). This surface plot further illustrates the interesting plateau and critical behavior of the negativity. It can be seen from Fig. (10) that for increasing  $|R|$  the negativity suddenly drops to zero at a critical  $R_c$  value, but it also drops to zero in the limit  $R \rightarrow 0$ . In this  $R \rightarrow 0$  limit, the negativity has a singularity since  $R$  values are chosen between interval  $-\pi \leq R \leq \pi$ . This Fig. (10) clearly demonstrates that the (symmetric positive and negative) critical  $R_c$  values are essentially independent of temperature  $T$ , although

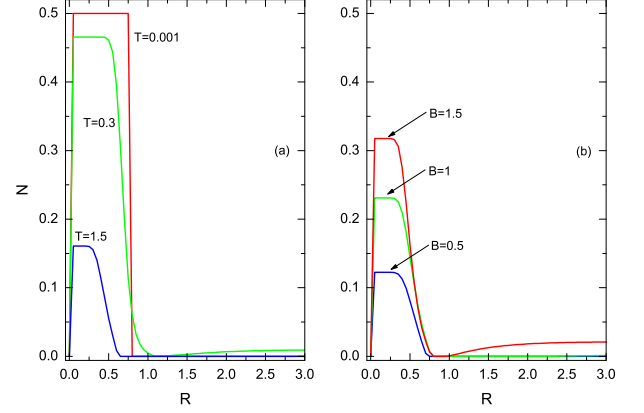


FIG. 9. Negativity as a function of  $R$  for the two-spin ferromagnetic XY model in the case  $J(R) = 1/\sinh^2 R$  (a) for selected temperatures at fixed  $B = 1$ , (b) for selected magnetic fields at fixed  $T = 1$ .

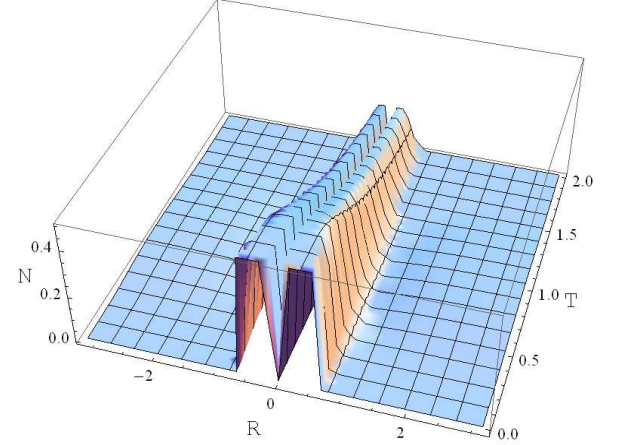


FIG. 10. Surface plot of the negativity for the two-spin ferromagnetic XY system in the case  $J(R) = 1/\sinh^2 R$  as a function temperature  $T$  and interaction parameter  $R$  at fixed  $B = 1.5$ .

the actual value of the negativity on the entanglement plateau does decrease with increasing  $T$ .

Finally, to further demonstrate and unify the dependence of entanglement on  $R$  and  $B$ , the negativity is plotted as a function  $R$  ( $-\pi \leq R \leq \pi$ ) and  $B$  for a fixed value  $T = 0.1$  in Fig. (11). Again plateau and critical behavior is apparent. It can be seen from Fig. (11) that the constant negativity on a plateau suddenly drops to zero at a critical  $R_c$  value. Here the (symmetric positive and negative)  $R_c$  show dependence on  $B$ , whereas—aside from the small  $B$  regime—the value of the negativity on the plateau is essentially saturated at  $N = 0.5$ . Similarly to Fig. (10), in the limit  $R \rightarrow 0$ , a singularity appears in the negativity since  $R$  values are chosen between interval

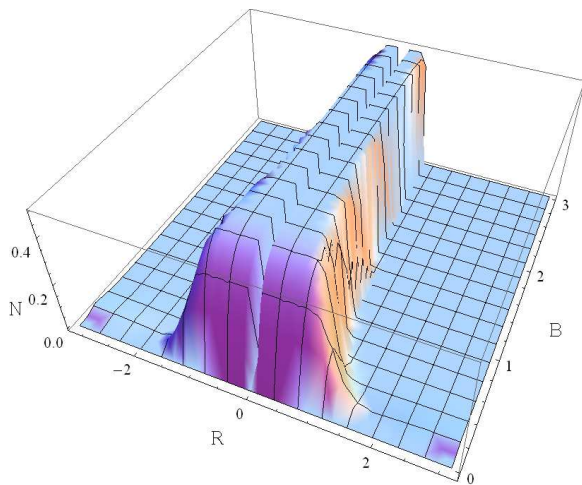


FIG. 11. Surface plot of the negativity for the two-spin ferromagnetic XY system in the case  $J(R) = 1/\sinh^2 R$  as a function magnetic field  $B$  and interaction parameter  $R$  at fixed  $T = 0.1$ .

$-\pi \leq R \leq \pi$ . In the small  $B$  regime the critical behavior disappears and the negativity decreases smoothly as the symmetric plateaus disappear for decreasing  $B$  or increasing  $R$ .

To summarize, in this final subsection, we have investigated the behavior of the entanglement of a two-spin XY system in the case of the long-range SCM interaction  $J(R) = 1/\sinh^2 R$ . We have also discussed the dependence of the negativity on interaction parameter  $R$ , magnetic field  $B$  and temperature  $T$ . We have demonstrated the symmetric behavior about  $R = 0$  (with singular behavior as  $R \rightarrow 0$ ). Critical plateau behavior is seen over a wide parameter regime along with the associated entanglement sudden death.

#### IV. CONCLUSIONS

In this study, using the concept of negativity we investigate entanglement in  $(1/2,1)$  mixed-spin XY models for the long-range interaction with an inverse-square and its trigonometric and hyperbolic variants given in the SCM model. We have also explored in detail the temperature and magnetic field dependence of the thermal entanglement in the  $(1/2,1)$  mixed-spin XY system for different

types of interactions. Our numerical results show that in the presence of the SCM type interactions characterized by an interaction parameter  $R$ , thermal entanglement between spin qubits has a rich behavior dependent upon  $R$ , the temperature  $T$  and the applied magnetic field strength  $B$ . Indeed, we have found that there are entanglement plateaus which saturate at the maximum negativity  $N = 0.5$  for significant regions of the parameter ranges of  $R$ ,  $T$  and  $B$ . Aside from specific examples, in general the entanglement plateaus are characterized by a critical distance  $R_c$  and moving off a plateau through  $R_c$  demonstrates a critical change and entanglement sudden death. Clearly the effect of SCM type interactions on the resource of entanglement provides a rich source of behavior, with maximum entanglement existing over significant parameter regimes and critical switching.

The plateau behaviors in entanglement formation of two-spin given by Eq. (1) for all types of SCM interactions are very interesting. The physical mechanism of entanglement plateaus probably may be long-range interactions. Indeed, while the plateau behavior in entanglement does not appear for short-range interactions, here, we can see that all long-range interactions with an inverse-square and its trigonometric and hyperbolic variants lead to different plateau behavior in the entanglement. Therefore, we can suggest that the plateau behavior of entanglement in these model emerge from the long-range character of the interactions. In all case for the long-range SCM interactions, entanglement between spins still subsists throughout plateau up to critical distance although spins are spatially separated from each other unlike the system with short-range interactions [67–70]. We believe that these interesting results can be valuable for researcher in this area of physics.

#### ACKNOWLEDGMENTS

This work was partially supported by YOK (The Council of Higher Education), the University of Leeds and TUBITAK (The Scientific and Technological Research Council of Turkey) under research project (No.109T681). The author (EA) gratefully acknowledges YOK, the University of Leeds, Istanbul University and TUBITAK. EA also gratefully acknowledges to Viv Kendon for invitation as a visitor to the Quantum Information Group (University of Leeds) where the first stages of this work were completed during the visit.

[1] M. A. Nielsen and I. A. Chuang, *Quantum Computing and Quantum Information* (Cambridge University Press, Cambridge, England, 2000)  
 [2] B. Schumacher, Phys. Rev. A **54**, 2614 (1996).  
 [3] C. H. Bennett, et al., Phys. Rev. Lett. **70**, 1895 (1993).  
 [4] C. H. Bennett and S. J. Wiesner, Phys. Rev. Lett. **69**, 2881 (1992).

[5] D. P. Divincenzo, Science **270**, 255 (1995).  
 [6] M. Christandl, N. Datta, A. Ekert and A. J. Landahl, Phys. Rev. Lett. **92**, 187902 (2004).  
 [7] A. K. Ekert, Phys. Rev. Lett. **67**, 661 (1991).  
 [8] D. Deutsch, et al., Phys. Rev. Lett. **77**, 2818 (1996).  
 [9] P. W. Shor, SIAM Journal on Computing **26**, 1484 (1997).



- [10] L. K. Grover, Phys. Rev. Lett. **79**, 325 (1997).
- [11] D. Loss and D. P. Divincenzo, Phys. Rev. A **57**, 120 (1998).
- [12] G. Bukard, D. Loss and D. P. Divincenzo, Phys. Rev. B **59**, 2070 (1999).
- [13] A. Imamoglu, et al., Phys. Rev. Lett. **83**, 4204 (1999).
- [14] P. M. Platzman and M. I. Dykman, Science **284**, 1967 (1999).
- [15] R. Raussendorf and H. J. Briegel, Phys. Rev. Lett. **86**, 5188 (2001).
- [16] S. Bose, J. Contemp. Phys. **48**, 13 (2007).
- [17] A. Kay, Int. J. Quantum Inf. **8**, 641 (2010).
- [18] G. L. Kamta and A. F. Starace, Phys. Rev. Lett. **88**, 107901 (2002).
- [19] Y. Yeo, Phys. Rev. A **66**, 062312 (2002).
- [20] G. L. Kamta, A. Y. Istomin and A. F. Starace, Eur. Phys. J. D. **44**, 389 (2007).
- [21] Y. Sun, Y. Chen and H. Chen, Phys. Rev. A **68**, 044301 (2003).
- [22] Y. Zhang, G.L. Long, Y. C. Wu and G. C. Guo, Commun. Theor. Phys. **47**, 787 (2007).
- [23] X. Wang, Phys. Rev. A **64**, 012313 (2001).
- [24] M. C. Arnesen, S. Bose and V. Vedral, Phys. Rev. Lett. **87**, 017901 (2001).
- [25] G. F. Zhang, Phys. Rev. A **75**, 034304 (2007).
- [26] M. Asoudeh, V. Karimipour, Phys. Rev. A **71**, 022308 (2005).
- [27] L. F. Santos, Phys. Rev. A **67**, 062306 (2003).
- [28] G. F. Zhang, S. S. Li, Phys. Rev. A **72**, 034302 (2005).
- [29] S. J. Gu, H. Q. Lin and Y. Q. Li, Phys. Rev. A **68**, 042330 (2003).
- [30] E. Albayrak, Eur. Phys. B **72**, 491 (2009); Opt. Commun. **284**, 1631 (2011)
- [31] E. Ercolessi, S. Evangelisti, F. Ravanini, Phys. Lett. A **374**, 2101 (2010).
- [32] J. M. Liu, P. F. Yu, J. G. Cai and G. T. Shen, Chin. J. Phys. **47**, 574 (2009).
- [33] L. Zhou, H. S. Song, Y. Q. Guo and C. Li, Phys. Rev. A **68**, 024301 (2003).
- [34] A. Abliz, et al., Phys. Rev. A **74**, 052105 (2006).
- [35] T. Chen, et al., Chin. Phys. B **19**, 050302 (2010).
- [36] D. C. Li and Z. L. Cao, Opt. Commun. **282**, 1226 (2009); Chin. Phys. Lett. **26**, 020309 (2009); Eur. Phys. J. D **50**, 207 (2008).
- [37] Z. Sun, et al., Physica A **370**, 483 (2006).
- [38] G. F. Zhang, S. S. Li and J. Q. Liang, Opt. Commun. **245**, 457 (2005).
- [39] G. F. Zhang, J. Q. Liang, G. E. Zhang and Q. W. Yan, Eur. Phys. J. D. **32**, 409 (2005).
- [40] C. Akyuz, E. Aydiner and O. E. Mustecaplioglu, Opt. Commun. **281**, 5271 (2008).
- [41] X. Wang and S. J. Gu, J. Phys. A Math. Theor. **40**, 10759 (2007).
- [42] X. Wang, H. B. Li, Z. Sun and Y. Q. Li, J. Phys. A Math. Gen. **38**, 8703 (2005).
- [43] B. Li and Y.-S. Wang, Physica B **407**, 77 (2011).
- [44] M. Gaudiano, O. Osenda and G. A. Raggio, Phys. Rev. A **77**, 022109 (2008).
- [45] D. Giuliano et al., New J. Phys. **12**, 025022 (2010)
- [46] F. Calogero, J. Math. Phys. (N.Y.) **10**, 2191 (1969); **10**, 2197 (1969); **12**, 419 (1971); **13**, 411 (1975); F. Calogero and C. Marchioro, Lett. Nuovo Cimento **13**, 383 (1975).
- [47] B. Sutherland, Phys. Rev. A **4**, 2019 (1971); **5**, 1375 (1972); **34**, 1083 (1975).
- [48] J. Moser, Adv. Math. **16**, 1 (1975).
- [49] J. Gibbons and T. Hermsen, Physica D **11**, 337 (1984).
- [50] S. Wojciechowski, Phys. Lett. A **111**, 107 (1985).
- [51] F. D. M. Haldane, Phys. Rev. Lett. **60**, 635 (1988).
- [52] B. S. Shastry, Phys. Rev. Lett. **60**, 639 (1988).
- [53] F. D. M. Haldane, Phys. Rev. Lett. **66**, 1529 (1991); F. D. M. Haldane et al. Phys. Rev. Lett. **69**, 2021 (1992); Z. N. C. Ha and F. D. M. Haldane, Phys. Rev. B **46**, 9359 (1992).
- [54] B. S. Shastry, Phys. Rev. Lett. **69**, 164 (1992).
- [55] N. Kawakami, Phys. Rev. B **46**, 1005 (1992); **46**, 3191 (1992).
- [56] K. Hikami and M. Wadati, Phys. Lett. A **173**, 263 (1993).
- [57] M. Fowler and J. A. Minahan, Phys. Rev. Lett. **70**, 2325 (1993).
- [58] B. Basu-Mallick, H. Ujino and M. Wadati, J. Phys. Soc. Jpn. **68**, 3219 (1999).
- [59] A. P. Polychronakos, Phys. Rev. Lett. **70**, 2329 (1993); Nucl. Phys. B **419** 553 (1994); Phys. Rev. Lett. **89**, 126403 (2002).
- [60] A. Peres, Phys. Rev. Lett. **77**, 1413 (1996).
- [61] M. Horodecki, et al., Phys. Lett. A **223**, 1 (1996).
- [62] G. Vidal and R. F. Werner, Phys. Rev. A **65**, 032314 (2002).
- [63] Ting Yu and J. H. Eberly, Phys. Rev. Lett. **93**, 140404 (2004).
- [64] J. H. Eberly and Ting Yu, Science **316**, 555 (2007).
- [65] Ting Yu and J. H. Eberly, Science **323**, 598 (2009).
- [66] Entanglement sudden death was first noted for evolution as a function of time. The usual use of this term applies to scenarios where the entanglement vanishes with a finite slope, rather than exhibiting an exponential or Gaussian decay, as a function of the relevant parameter.
- [67] L. C. Venuti, C. D. E. Boschi and M. Roncaglia, Phys. Rev. Lett. **96**, 247206 (2006).
- [68] T. J. Osborne and M. A. Nielsen, Phys. Rev. A **66**, 032110 (2002).
- [69] A. Osterloh, L. Amico, G. Falci, and R. Fazio, Nature (London) **416**, 608 (2002).
- [70] B.-Q. Jin and V. E. Korepin, Phys. Rev. A **69**, 062314 (2004).